

PAPER • OPEN ACCESS

A New Correlation between Galaxy Stellar Masses and Spiral Arm

To cite this article: Ismaeel A. Al-Baidhany *et al* 2019 *J. Phys.: Conf. Ser.* **1234** 012015

View the [article online](#) for updates and enhancements.



IOP | ebooks™

Bringing you innovative digital publishing with leading voices to create your essential collection of books in STEM research.

Start exploring the [collection](#) - download the first chapter of every title for free.

A New Correlation between Galaxy Stellar Masses and Spiral Arm

Ismaeel A. Al-Baidhany¹, Sami Salman Chiad¹, Wasmaa A. Jabbar¹, Nadir Fadhil Habubi^{1*}, Tahseen H. Mubarak², Abdulhussain Abbas Khadayeir³, Ehssan S. Hassan⁴, Mohamed Odda Dawod⁴ and Khalid Haneen Abass⁵

¹Department of Physics, College of Education, Mustansiriyah University, Baghdad, Iraq.

²Department of Physics, College of Science, University of Diyala, Iraq.

³Department of Physics, College of Education, University of Al-Qadisiyah, Iraq.

⁴Department of Physics, College of Science, Mustansiriyah University, Baghdad, Iraq.

⁵Department of Physics, College of Education for Pure Sciences, University of Babylon, Iraq.

E-mail: ismaeel_2000@uomustansiriyah.edu.iq, dr.sami@uomustansiriyah.edu.iq, wasmaajabbar@uomustansiriyah.edu.iq, nadirfadhil@uomustansiriyah.edu.iq, abdulhussain.khadayair@qu.edu.iq, dean@sciences.uodiyala.edu.iq, pure.khalid.haneen@uobabylon.edu.iq, mohammedodda2017@uomustansiriyah.edu.iq, ehsanphysician@uomustansiriyah.edu.iq.
***Corresponding Author. E-mail:** nadirfadhil@uomustansiriyah.edu.iq.

Abstract: We present a new relation between pitch angle of spiral arm (a parameter of the tightness of spiral structure) and the galaxy stellar masses.

Taken both with the result that stellar mass seems to determine pitch angle of spiral arm, one would anticipate a correlation to exist between pitch angle of spiral galaxy and the galaxy stellar masses in disk of spiral galaxies.

In this study, we measured the stellar mass of galaxy by using the calibration of $L_{3.6\mu\text{m,gal}}$ and using the constant mass-to-light ratio $(M/L)_{3.6\mu\text{m,gal}}$, were derived from the stellar population models. We conclude that pitch angle of spiral arm is a instrument to calculate indirect measurements of the stellar mass of galaxy.

Key words: subject headings: Galaxies: disk galaxies - Galaxies: spiral galaxies - Galaxies: stellar mass - Galaxies: spiral arm pitch angle.

1. Introduction:

That often need to measure in astrophysics is the stellar mass and the pitch angles of spiral arm in spiral galaxies.

Although it is to measure the stellar mass of galaxy. In addition, one can measure the total stellar mass by kinematics, but it is the mass of stars [1].



Models of photometry used in optical, infrared spectra to provide the measurements of the surface brightness or luminosity of spiral galaxies [2].

By using and GALEX data, Fisher et al. (2009) [3] showed that pseudobulges are increasing the B/T (bulge-to-total mass ratio) via internal star formation in bulges. As well, they pointed out star formation averages are high enough to account for the entire stellar mass of pseudobulges galaxies [3]. These authors also found that star formation density, which played an important role in the growth or formation of pseudobulges [4]. showed that the average B/T of classical bulges (0.4) is higher than that of pseudobulges (0.16).

Over the last decade, studies of galaxies have led to the discovery that there are many strong correlations between the mass and the properties of the spheroid components of the spiral hosts galaxies. This an evidence that a correlation to exist between the formation of galaxy and growth of SMBH in the center of galaxy [5]. As a result, astronomers think that the energy emitted by growing SMBHs shaping the properties of the structure of their host spiral galaxies [6].

There is increasing guides which indicates that correlations between the SMBH masses and an assortment of host galaxy (bulge) parameters

In this work: First, the stellar masses galaxies in 32 galaxies are measured using the calibration from $L_{3.6\mu\text{m,gal}}$ and using constant mass-to-light ratio $(M/L)_{3.6\mu\text{m,gal}}$. Second, the pitch angle of spiral arm estimated using a two-dimensional fast Fourier Transform (2FFT) [7]. Finally, the data obtained were used in Table (2) to find new relations between the stellar masses galaxies ($M_{3.6,gal}$), and spiral arm pitch angles.

2. Measurement

2.1 Measurement of the galaxy luminosity ($L_{3.6,gal}$):

The measurement of the bulge luminosity is based on a two-dimensional (bulge - bar - disk) decomposition program to model Spitzer/IRAC 3.6 μm images. The bulge luminosity was determined for a sample of 32 spiral galaxies by applying the two-dimensional multicomponent decomposition method. In this method, an exponential function was used to describe the disc:

$$I_d(r) = I_{od} \exp[-(r/h_r)],$$

where I_{od} is the central surface density of the disc, h_r is the radial scalength of the disc, and r is disc radius.

The orientation parameters were estimated using Spitzer/IRAC 3.6 μm images of 32 galaxies with spiral arm pitch angle estimates.

These images were used to measure the minor-to-major axis ratios ($q = b/a$), effective radii (R_e), the radial profiles of the isophotal major-axis position angles (φ) and the estimated inclinations of the disk using the mean values in the outer parts of the disks.

First, foreground stars were removed and all point sources from the Spitzer 3.6 μm images were masked out by using SExtractor (Bertin & Arnouts 1996), Next, the surface brightness profiles were derived using the ELLIPSE routine in IRAF [8] To change surface brightness units to mag arcsec^{-2} , the following formula was used:

$$\mu_{3.6\mu\text{m}} = -2.5 \times \log_{10} \left[\frac{S_{3.6\mu\text{m}} \times 2.35 \times 10^{-5}}{ZP_{3.6\mu\text{m}}} \right], \quad (1)$$

Where $S_{3.6\mu\text{m}}$ is the flux value of the 3.6 μm band in units of MJy sr^{-1} , $ZP_{3.6\mu\text{m}}$ is the IRAC zero magnitude flux density in Jy and is 280.9. Apparent magnitude was converted to absolute magnitude was convert using luminosity distance and absorption in the galaxies according to the NED database.

2.2 Measurement of the stellar mass ($M_{3.6,\text{gal}}$):

Marconi et al. [9], and Sani et al. [10] used the J, I, and K band luminosity to compute stellar mass by assuming a mass-to-light ratio $M/L = 1$. Bell & de Jong found a relation between optical colors (e.g., B-R, B-V) and the near-infrared stellar mass-to-light (M/L or γ) ratio of disk galaxies [11].

These previous studies of optical colors of disk galaxies do not provide the γ values for the Spitzer/IRAC bands, so they cannot be used here. Therefore, a new relation was used to obtain γ in the 3.6- μm Spitzer/IRAC. This relation is between γ^K and γ in the 3.6- μm waveband was reported by Se-Heon Oh et al. (2008) [12]:

$$\gamma^{3.6} = B^{3.6} \times \gamma^K \times A^{3.6} \quad (2)$$

Where $A^{3.6} = -0.05$ and $B^{3.6} = 0.92$

A relation between the (γ^K) and optical colors is given by,

$$\text{Log}_{10}(\gamma^K) = b^K \times \text{Optical colors} + a^K \quad (3)$$

Where a^K and b^K are coefficients for the relation between γ^K and the optical colors given in Bell & de Jong (2001) [11]. By combining Equation (1) with Equation (2), adopting 20% [23], using the optical colors given in Bell & de Jong (2001) [11] and a scaled cutting off the stars than $\sim 0.35 M$ [11], the 3.6 μm M/L ratio was calculated.

2.3 Measuring spiral arm pitch angle

Previous studies described a logarithmic spiral in polar coordinates [13-21]. This is a the special kind of spiral curve that describes the arm in disk galaxies:

$$r = r_0 e^{\theta \tan(\Phi)} \quad (4)$$

where r is radius, θ is central angle, r_0 is initial radius when $\theta = 0$, and pitch angle is $-90 \leq \Phi \leq 90$.

Because the spiral arm pitch angle has been shown to be independent of the wavelength at which it is measured, multi-band images were used to determine it for our sample of spiral galaxies [19].

Spiral arm pitch angles were measured using a two-dimensional fast Fourier transform (2DFFT) decomposition with logarithmic spirals of Spitzer 3.6 μm images of 32 galaxies, with inclinations of $30^\circ \leq i \leq 60^\circ$. The 2DFFT program analyzes images of spiral galaxies and categorizes their pitch angles and number of arms. The two-dimensional fast Fourier transform decomposition program is fully described by I. Puerari in Schröder [7].

The amplitude of each Fourier component is given by:

$$A(m,p) = \frac{\sum_{i=1}^l \sum_j^l I_{ij}(\ln r, \theta) \exp[-i(m\theta + p * \ln r)]}{\sum_{i=1}^l \sum_j^l I_{ij}(\ln r, \theta)} \quad (5)$$

where r and θ are polar coordinates, $I(\ln r, \theta)$ is the intensity at position $(\ln r, \theta)$, m represents the number of arms or modes, and p is the variable associated with the pitch angle P defined by $P = -(m/p_{\text{max}})$.

was used to determine the ellipticity values and major-axis position angle to order to deproject the 3.6 μm galaxy images to fully face-on by assuming circular outer isophotes. in IRAF was used to derive inclination angle (α); [22,8], which is defined by:

$$\alpha = \cos^{-1}(b/a) \quad (6)$$

Where (a) is the semi-major axis and (b) is the semi-minor axis. Where the value 0° describes a face-on galaxy and 90° describes an edge-on galaxy,

3. Results and discussions

Lists the pitch angle of spiral arm, stellar mass galaxies, respectively. From galaxy stellar mass-to-light ratios, we derive galaxy stellar mass respectively. We determined model-disc luminosities using the flux density. In addition, we calculated the absolute magnitudes using distance modulus and the apparent magnitudes.

By analyzing the sample of 32 spiral galaxies and plotting of the $M_{3.6,\text{gal}} - P$ correlation, we concluded there is a relation between $M_{3.6,\text{gal}}$ and P . In Table (2), we list the parameters of the best-fitting lines shown for this diagram.

Figure (1) illustrates the relations in $M_{3.6,\text{gal}}$ -spiral arm pitch angle (we assigned a particular marker to these galaxies according to their morphological bulge type- i.e. bulge and pseudobulge galaxies in Figure (2) was noted that both pseudobulges and bulges galaxies are located between the fitting line. The best-fitting lines are shown for this diagram:

$$\log_{10} M_{3.6,\text{gal}} = (11.68 \pm 0.93) - (0.067 \pm 0.017)P \quad (7)$$

Pearson's linear coefficient is 0.81 for classical bulges and pseudobulges. This means a strong correlation exists between stellar masses and pitch angle of spiral arm in late-type galaxies.

Figure (3) shows the correlation of the pitch angle with stellar masses distribution for the sample of galaxies described bulge in Table (2), where the scatter looks somewhat large in the $M_{3.6,gal} - P$ relation.

Based on the conclusion of many of researchers [24, 25]. The $M_{3.6,gal} - V, \sigma$ relations and our relation ($M_{3.6,gal} - P$) supports the concept of regulated formation mechanisms and co-evolution for the stellar mass of galaxies. (biggest structures in galaxy) and the pitch angle of galaxies.

In figure (2), we have recomputed them, especially for pseudobulges with $n \leq 2$, to get more accurate results.

The brightness profiles for spiral galaxies that would dilute the dilute in the structure of galactic spiral, where stellar light in the spiral structure strongly depends at the large radii of galaxy's disc in addition, the spiral structure little depends on disc's radius which is basically of the pseudobulge participates.

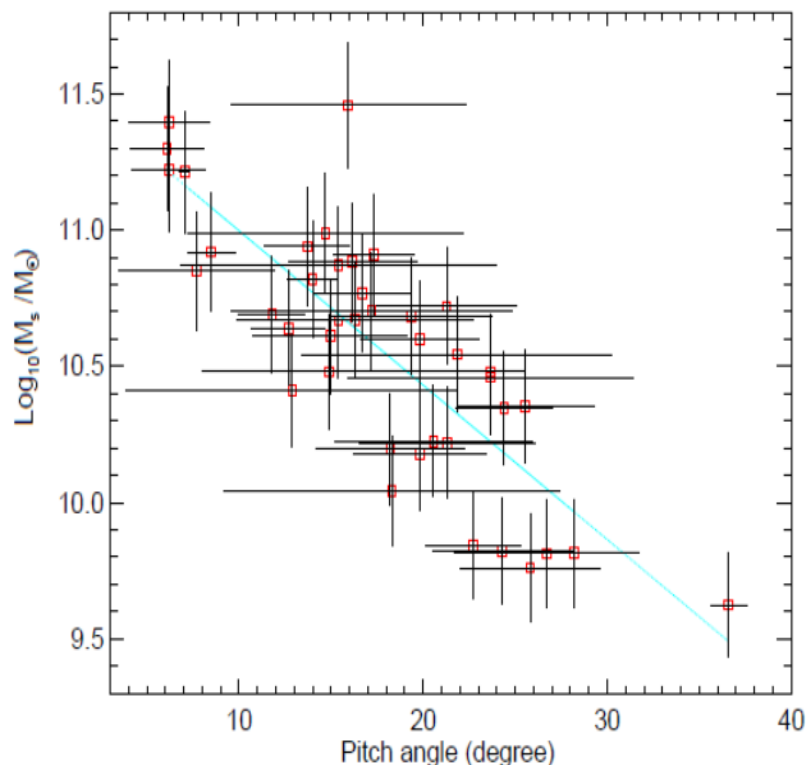


Figure 1. Stellar masses galaxies ($M_{3.6,gal}$) as a function of the spiral arm pitch angle. The solid line is the fit to all spiral galaxies.

The fundamental $M_{3.6,gal} - P$ scaling relations of spiral galaxies were examined taking into consideration the kind of the bulge (classical bulges or pseudobulges). Figure (2) illustrates

the relations in $M_{3.6,gal.}$ - P , where the classical bulges and pseudo-bulges have prominent correlations. The best-fitting lines are shown for this diagram:

$$\log_{10} M_{3.6,gal.} = (11.7 \pm 0.5) - (0.035 \pm 0.02)P \quad \text{pseudobulges} \quad (8)$$

$$\log_{10} M_{3.6,gal.} = (11.31 \pm 0.31) - (0.053 \pm 0.015)P \quad \text{classical bulges} \quad (9)$$

Pearson's linear coefficient for a relation between $M_{3.6,gal.}$ and P are 0.85, and 0.79 for classical bulges and pseudobulges, respectively. We note that Pearson's linear coefficient values for two types of the bulge (classical bulges or pseudobulges) of spiral galaxies are shown to have a strong correlation. These results have a significance of 99.6%, a 3σ result.

As well, Figure (2) illustrates that there is a correlation between the $M_{3.6,gal.}$ and the spiral arm pitch angle: galaxies with high stellar mass galaxy have smaller pitch angles. The relation looks somewhat good for pseudobulges with $n \leq 2$. In addition, pseudobulges with small pitch angle follow the same scaling relations as classical bulges, while those with large pitch angle deviate from the scaling relations of classical bulges.

The pitch angle–stellar mass galaxy relations (non-barred, AGN, and non-AGN galaxies) (Figure (3)) show the same behaviour. There is a significant correlation between the pitch angles and the galaxies stellar masses for all of them.

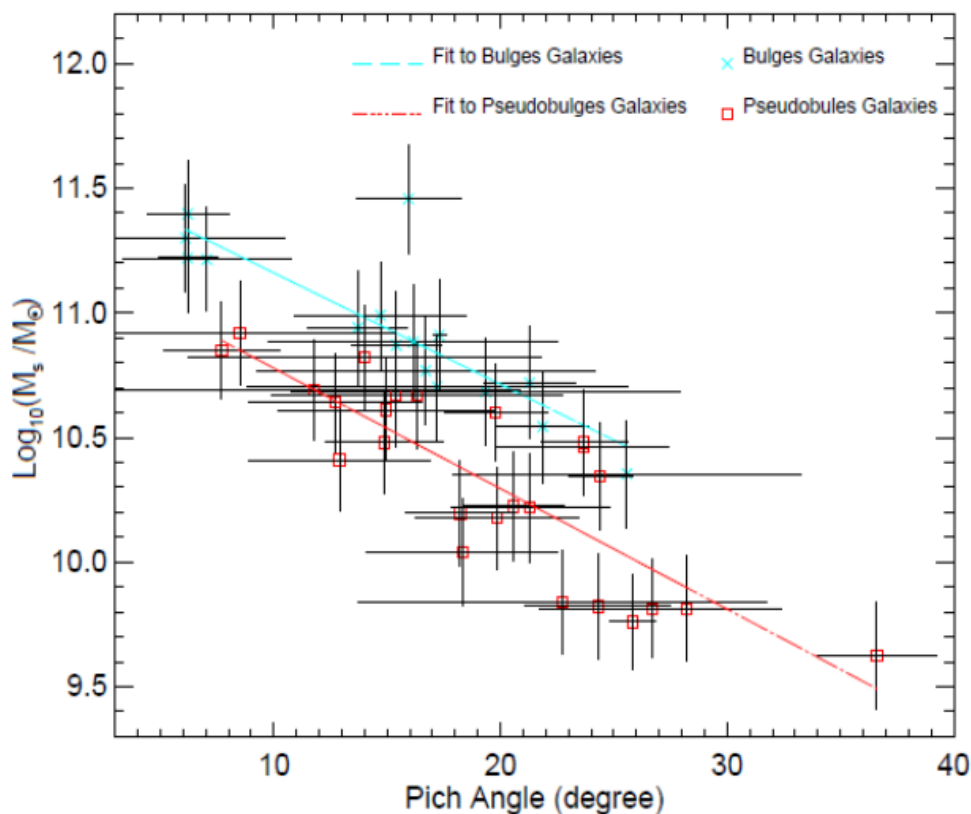


Figure 2. Galaxy stellar mass ($M_{3.6,gal.}$) as a function of spiral arm pitch angle. The linear regressions are shown as dashed, and dash-dot respectively, for classical bulges.

Figure (3) shows a plot of SMBH masses from the ($M_{3.6,gal}$ -P) relation, for non-barred, non-AGN, and AGN galaxies, respectively. Pearson's linear coefficient for a relation between $M_{3.6,gal}$ and P is 0.79, 0.82, and 0.78 for non-barred, non-AGN, and AGN galaxies, respectively.

The slope of the $M_{3.6,gal}$ -P relation in the AGNs is somewhat low compared to non-barred, non-AGN. Pearson's linear coefficient values for all types of galaxies were noted to have level of the significance at which the null hypothesis of zero correlation is disproved at 3σ . The best-fitting lines are shown for this diagram:

$$\log_{10} M_{3.6,gal.} = (11.61 \pm 0.5) - (0.061 \pm 0.02)P \quad (\text{Non-Barred}) \quad (10)$$

$$\log_{10} M_{3.6,gal.} = (11.73 \pm 0.3) - (0.07 \pm 0.008)P \quad (\text{Non-AGN}) \quad (11)$$

$$\log_{10} M_{3.6,gal.} = (11.52 \pm 0.4) - (0.043 \pm 0.006)P \quad (\text{AGN}) \quad (12)$$

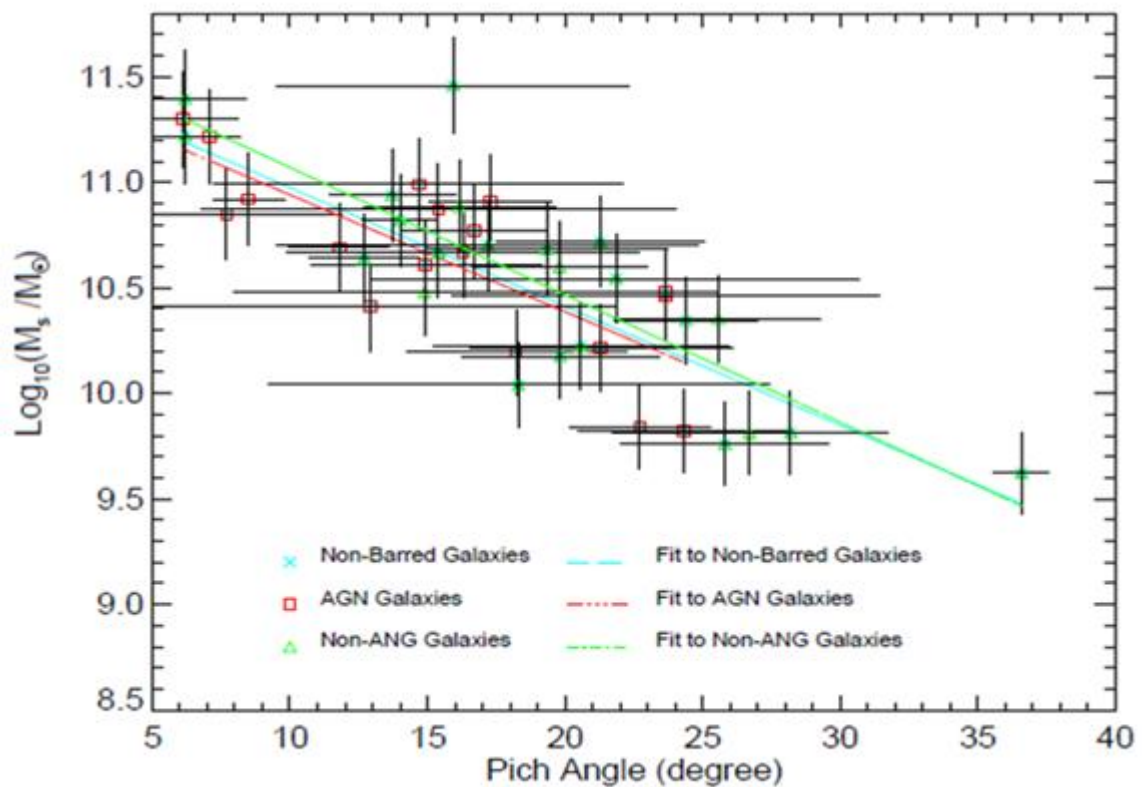


Figure 3. Galaxy stellar mass ($M_{3.6,gal.}$) as a function of the spiral arm pitch angle. The linear regressions are shown as long dash, dash dot dot dot, dash dot and dashed , respectively, for , non-barred, non-AGN, and AGN galaxies.

Table 1. Linear correlation coefficient and linear regression coefficients of galaxy stellar mass as a function of the spiral arm pitch angle.

Types of galaxies	α	β	No. of galaxies	correlation coefficient
All galaxies	11.68 ± 0.93	0.067 ± 0.017	32	0.81
Pseudo bulges galaxies	11.7 ± 0.5	0.035 ± 0.020	17	0.85
Classical Bulges galaxies	11.31 ± 0.31	0.053 ± 0.015	14	0.79
Non-Barred galaxies	11.61 ± 0.50	0.061 ± 0.020	13	0.79
AGN galaxies	11.73 ± 0.30	0.070 ± 0.008	12	0.82
Non-AGN galaxies	11.52 ± 0.40	0.043 ± 0.006	20	0.78

Table (2). The properties for spirals of Spitzer/IRAC 3.6 μm images of 32 galaxies.

galaxy (1)	Leda Type (2)	P (deg.) (3)	$M_s(M_\odot)$ (4)	B or nB (5)	AGN or AGN (6)	C or P (7)
IC 2560	SBb	$16.5 \pm 3.53^{(3)}$	10.9 ± 0.2	B	AGN	P
NGC 613	Sbc	$21.57 \pm 1.77^{(1)}$	10.6 ± 0.5	nB	AGN	P
NGC 1022	SBa	$19.83 \pm 3.6^{(1)}$	10.12.14	B	nAGN	P
NGC 1068	Sb	$17.3 \pm 2.2^{(2)}$	11.4 ± 0.1	nB	AGN	P
NGC 1097	SBb	$16.7 \pm 2.62^{(3)}$	10.9 ± 0.4	B	AGN	P
NGC 1300	Sbc	$12.71 \pm 1.99^{(1)}$	10.8 ± 0.1	nB	nAGN	P
NGC 1350	Sab	$20.57 \pm 5.38^{(1)}$	10.7 ± 0.1	nB	nAGN	P
NGC 1353	Sb	$32.37 \pm 5.4^{(1)}$	9.72 ± 0.3	nB	nAGN	P
NGC 1357	Sab	$16.16 \pm 3.48^{(1)}$	10.6 ± 0.2	nB	nAGN	P
NGC 1365	Sb	$15.4 \pm 2.4^{(3)}$	10.5 ± 0.2	B	nAGN	P
NGC 1398	SBab	$6.2 \pm 2^{(3)}$	10.11 ± 0.1	B	nAGN	C
NGC 1433	SBab	$25.82 \pm 3.79^{(1)}$	10.5 ± 0.4	B	nAGN	C
NGC 1566	SABb	$21.31 \pm 4.78^{(3)}$	9.88 ± 0.3	B	AGN	P
NGC 1672	Sb	$18.22 \pm 14.07^{(3)}$	9.98 ± 0.3	nB	AGN	C
NGC 1808	Sa	$23.65 \pm 7.77^{(1)}$	10.4 ± 0.1	nB	AGN	P
NGC 2442	Sbc	$14.95 \pm 4.2^{(1)}$	10.6 ± 0.4	B	AGN	P
NGC 3511	SABc	$28.21 \pm 2.27^{(1)}$	9.78 ± 0.1	B	nAGN	P
NGC 3521	SABb	$19.16 \pm 6.34^{(3)}$	10.7 ± 0.4	B	nAGN	C
NGC 3673	Sb	$19.34 \pm 4.38^{(1)}$	10.5 ± 0.1	nB	nAGN	C

NGC 3783	SBab	22.73±2.58	9.72±0.2	B	AGN	C
NGC 3887	Sbc	24.4±2.6 ⁽²⁾	9.83±0.3	nB	nAGN	P
NGC 4030	Sbc	19.8±3.2 ⁽²⁾	10.12±0.3	nB	nAGN	P
NGC 4462	SBab	15.32±5.42 ⁽¹⁾	10.8±0.2	B	nAGN	C
NGC 4699	SABb	6.2±2.2 ⁽¹⁾	10.9±0.2	B	nAGN	C
NGC 5054	Sbc	25.57±3.73 ⁽¹⁾	10.4±0.3	nB	nAGN	C
NGC 6300	SBb	24.3±3.8 ⁽¹⁾	10.2±0.053	B	AGN	P
NGC 6744	SABb	21.28±3.8 ⁽¹⁾	10.5±0.5	B	nAGN	C
NGC 6902	SBab	13.71±2.3 ⁽³⁾	10.7±0.5	B	nAGN	C
NGC 7213	Sa	7.05±0.28 ⁽¹⁾	10.11±0.4	nB	AGN	C
NGC 7531	SABb	18.31±9.09 ⁽¹⁾	10.5±0.5	B	nAGN	C
NGC 7582	SBab	14.66±7.44 ⁽³⁾	10.11±0.5	B	AGN	C
NGC 7727	SABa	15.94±6.39 ⁽¹⁾	11.3±0.4	B	nAGN	C

Col. (1), of the galaxies; Col. (2), Hubble type taken from the HyperLeda catalogue; Col. (3), spiral arm pitch angle taken from Col. (4), stellar masses; Col. (5), B-Barred galaxy; nB - Non-Barred galaxy; Col. (6) AGN and non-AGN; Col. (7), C – classical bulge ; P - pseudobulge.

4. Conclusion

1- that spiral arm pitch and the galaxy stellar masses regulate each other. That means that mass of the pitch angle of spiral arm is somehow tied to the structural parameters of the rest of the galaxy .

2- Scaling relations were studied between the galaxy stellar masses ($M_{3.6,gal.}$), and pitch angles of spiral arm. The galaxy stellar masses were determined based on the luminosity of 3.6 μ m Spitzer/IRAC images of 32 spiral galaxies, and the best-fitting lines regressions were:

$$\log_{10} M_{3.6,gal.} = (11.68 \pm 0.93) - (0.067 \pm 0.017)P$$

$$\log_{10} M_{3.6,gal.} = (11.7 \pm 0.5) - (0.035 \pm 0.02)P \quad \text{pseudobulges}$$

$$\log_{10} M_{3.6,gal.} = (11.31 \pm 0.31) - (0.053 \pm 0.015)P \quad \text{classical bulges}$$

$$\log_{10} M_{3.6,gal.} = (11.61 \pm 0.5) - (0.061 \pm 0.02)P \quad (\text{Non - Barred})$$

$$\log_{10} M_{3.6,gal.} = (11.73 \pm 0.3) - (0.07 \pm 0.008)P \quad (\text{Non - AGN})$$

$$\log_{10} M_{3.6,gal.} = (11.52 \pm 0.4) - (0.043 \pm 0.006)P \quad (\text{AGN})$$

Acknowledgments:

The authors would like to thank the Mustansiriyah University (www.mustansiriyah.edu.iq) Baghdad- Iraq for its support of this work.

References

- [1] Bekerait'e S Walcher C J Wisotzki L Croton D Falc'on-Barroso J Lyubenova M Obreschkow D S'anchez S F Spekkens K Torrey P van de Ven G Zwaan M A Ascasibar Y Bland-Hawthorn J Gonz'alez Delgado R Husemann B Marino R A Vogelsberger M and B Ziegler 2016 ApJ. **827**, L36.
- [2] Oldham L J and Auger M W 2018 MNRAS **476** 133.
- [3] Fisher D B Drory N and Fabricius, M 2009 Ap. J. **697** 630.
- [4] Fisher D B and Drory N 2008 AJ. **136** 773.
- [5] Yuexing L I and Lars Hernquist 2007arXiv:astro-ph/0608190
- [6] Benson A J and Bower R 2010 MNRAS **405** 1573-1623.
- [7] Schröder M F Pastoriza M G Keple S O and Puerari I 1994 A&AS **108** 41.
- [8] Jedrzejewski R I 1987 MNRAS **226** 747.
- [9] Marconi A and Hunt L K 2003 ApJ. **589** L21–L24
- [10] Sani E Marconi A Hunt L Kand Risaliti G 2011 MNRAS **413** 1479-94.
- [11] Bell E F and de Jong R S 2001 ApJ. **550** 212.
- [12] Se-Heon Oh et al. 2008 arXiv: **0810** 2119.
- [13] Lin C. C and Shu F H 1964 ApJ. **140** 646.
- [14] Kennicutt R C 1981 AJ. **86** 1847.
- [15] Elmegreen B G Elmegreen D M and Hirst A C2004 ApJ. **612** 191.
- [16] Seigar M S and James P A 1998 MNRAS **299** 672.
- [17] Seigar M S and James P A 1998 MNRAS **299** 68532 1391.
- [18] Seigar M S Block D L Puerari I and Chorney N E 2005 MNRAS **59** 1065.
- [19] Seigar M S Bullock J S Barth A J and Ho L C 2006 ApJ. **645** 1012.
- [20] Seigar M S Ho L C and Barth AJ 2006 Bulletin of the AAS **38** 1190.
- [21] Vallée J P 2002 ApJ. **566** 261-266.
- [22] Hubble E P 1926, ApJ. **64** 321.
- [23] Ferrarese L 2002 ApJ. **578** 90–97.
- [24] Hu J 2009 ArXiv. **0908**.2028.
- [25] Al-Baidhany I Rashid. H G Chiad S S Habubi N F Jandow N N Jabbar W A and Abass k H 2018 IOP Conf. Series: Journal of Physics: Conf. Series **1003** 012107.